High mobility transparent thin-film transistors with amorphous zinc tin oxide channel layer

H. Q. Chiang[a)] and J. F. Wager
School of Electrical Engineering and Computer Science, Oregon State University, Corvallis, Oregon 97331-3211

R. L. Hoffman
Hewlett-Packard Company, 1000 NE Circle Boulevard, Corvallis, Oregon 97330-4239

J. Jeong and D. A. Keszler
Department of Chemistry, Oregon State University, Corvallis, Oregon 97331-4003

Transparent thin-film transistors (TTFTs) with an amorphous zinc tin oxide channel layer formed via rf magnetron sputter deposition are demonstrated. Field-effect mobilities of 5–15 and 20–50 cm^2 V^{-1} s^{-1} are obtained for devices post-deposition annealed at 300 and 600 °C, respectively. TTFTs processed at 300 and 600 °C yield devices with turn-on voltage of 0–15 and −5–5 V, respectively. Under both processing conditions, a drain current on-to-off ratio greater than 10^7 is obtained. Zinc tin oxide is one example of a new class of high performance TTFT channel materials involving amorphous oxides composed of heavy-metal cations with $(n-1)d^{10}$ ns^0 ($n \geq 4$) electronic configurations. © *2005 American Institute of Physics*. [DOI: 10.1063/1.1843286]

The recent development of transparent thin-film transistors (TTFTs)[1–6] represents a major advance in the emerging field of transparent electronics. These transistors have been fabricated on the basis of crystalline oxide channels that are typically produced at relatively high processing temperatures. To appraise the potential for reducing these temperatures, while retaining or improving transistor performance, we have examined the use of amorphous channel materials. Here, we describe an example of a high-performance TTFT having an amorphous oxide channel.

Amorphous oxides composed of heavy-metal cations with $(n-1)d^{10}$ ns^0 ($n \geq 4$) electronic configurations constitute an interesting class of transparent conductors, since they possess relatively high electron mobilities despite their amorphous character.[7–9] Examples of such materials include indium oxide doped with tin (ITO)[10] and zinc tin oxide[11] for which amorphous-state mobilities as large as 40 and 30 cm^2 V^{-1} s^{-1}, respectively, have been reported. Such high mobilities in an amorphous material are likely a consequence of a conduction band primarily derived from spherically symmetric, heavy-metal cation ns orbitals. Such orbitals have large radii, leading to a high degree of overlap between adjacent orbitals and considerable band dispersion. Moreover, the spherical symmetry of an s orbital makes delocalized electronic transport less sensitive to local and extended structural order as compared with band formation from anisotropic p or d orbitals. Furthermore, multicomponent oxide semiconductors are preferred to binary oxides for ensuring that the structure remains amorphous under a range of processing conditions.

Zinc tin oxide[11–19] is a wide band gap, n-type semiconductor; its stoichiometry can be most generally described as $(ZnO)_x(SnO_2)_{1-x}$ ($0 < x < 1$). Two crystalline forms have been reported, trigonal ilmenite $(ZnSnO_3)$[15] and cubic spinel (Zn_2SnO_4).[18] The ilmenite phase exhibits limited thermal stability.[12,13,15] In bulk samples, decomposition of $ZnSnO_3$ to Zn_2SnO_4 and SnO_2 has been noted at temperatures as low as 600 °C,[15] but the rate of this process is rather slow.

Zinc tin oxide thin films have been primarily investigated for transparent conductor applications.[11–18] Thin films typically exhibit a direct optical band gap of 3.3–3.9 eV. This broad band gap range likely arises from a combination of a large Burstein–Moss shift and compositional or structural variations of the zinc tin oxide thin films; the fundamental band gap of Zn_2SnO_4 has been reported to be 3.35 eV.[18] Attractive attributes of zinc tin oxide include its chemical stability with respect to oxidation and etching,[13,17] its physical robustness and extreme resistance to scratching,[17] and its tendency to possess an exceedingly smooth surface in thin films.[17,18]

Zinc tin oxide TFTs are fabricated here using two similar bottom-gate test structures, the first employing a glass substrate for realization of fully transparent devices and the second employing a heavily doped Si wafer with a SiO$_2$ gate dielectric layer formed via thermal oxidation. The description provided here deals explicitly with the transparent structure; the oxidized Si structure differs only in the nature of the gate dielectric and electrode. The electrical performance characteristics of the transparent and the Si-substrate structures are similar, although the Si-substrate devices exhibit less device-to-device and substrate-to-substrate variability.

TTFTs are prepared on Nippon Electric Company glass substrates (NEG OA2) coated with a 200-nm sputtered ITO gate electrode film and a 220-nm atomic layer deposited superlattice of AlO$_x$ and TiO$_x$ (ATO).[20] The zinc tin oxide channel layer (typically ~20–90 nm) and ITO (typically ~250 nm) source and drain electrodes are deposited via rf magnetron sputtering in Ar/O$_2$ (90%/10%) and Ar (100%), respectively, at a substrate temperature of ~175 °C. Zinc-tin-oxide films are deposited with a target fabricated in the Oregon State University Department of Chemistry (a mixture of ZnO and SnO$_2$ powder with a ZnO:SnO$_2$ molar ratio of
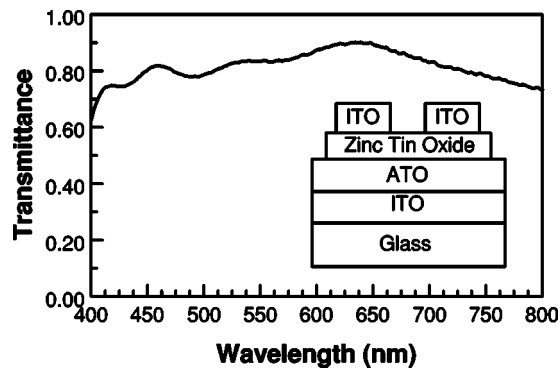

[a)]Electronic mail: chiang@ece.orst.edu

FIG. 1. Optical transmittance as viewed through the source/drain region (~84% in the visible portion of the electromagnetic spectrum) of a zinc tin oxide channel TTFT. (Inset) Prototypical TTFT device structure.

FIG. 3. Representative $\log(I_D)-V_{GS}$ and $\log(I_G)-V_{GS}$ characteristics (V_{DS} =40 V) for zinc tin oxide (sputter deposited from a $ZnSnO_3$ target) TTFTs annealed at 600 °C. Inset shows I_D-V_{DS} characteristic (V_{GS} is varied from 3 to 15 V in 3 V steps and I_D increases with increasing V_{GS}).

1:1 is sintered overnight at 1100 °C) and with several targets purchased from a commercial supplier ($ZnO:SnO_2$ molar ratios of 2:1 and 1:1). Devices are typically furnace annealed in air at 300 or 600 °C for 1 hour following zinc tin oxide deposition. The complete staggered, bottom-gate device structure is shown in the inset of Fig. 1. Six devices with W/L=7100 μm/1500 μm (~4.7/1) 1 in.×1 in. substrate. Channel and source/drain electrode layers are patterned through the use of shadow masks.

The zinc tin oxide thin films described here, as TTFT channel layers, are essentially amorphous. X-ray diffraction (XRD) patterns are obtained from two systems; the results from these systems vary slightly. The first system is a Philips MRD instrument that employs Cu $K\alpha$ radiation (0.5° incident angle); the XRD patterns from this system exhibit a single, extremely broad peak at $2\theta \sim 34°$, characteristic of amorphous zinc tin oxide films previously reported in the literature.[11,17,18] The second system is a Rigaku rapid image-plate machine with Cu $K\alpha$ radiation (10° incident angle) provided by a rotating anode and a 0.5-mm pinhole collimator; an XRD pattern obtained from this system is shown in Fig. 2 and is representative of zinc tin oxide films that are prepared by using a $ZnSnO_3$ target with annealing treatments up to 600 °C. Broad XRD profiles are observed at 2θ values near 34°, 59°, and 90°.[17] These bands encompass the major diffraction peaks for both ilmenite $ZnSnO_3$ and spinel Zn_2SnO_4,
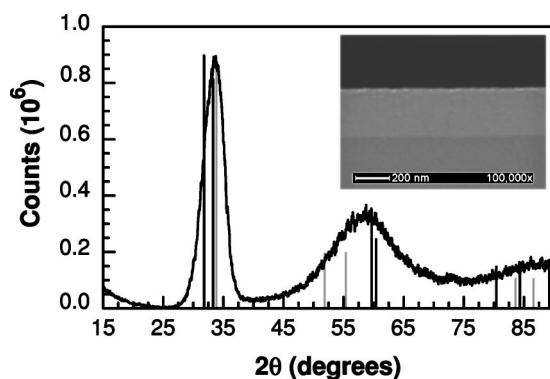

FIG. 2. XRD pattern obtained from an ~200-nm zinc tin oxide thin film deposited from a target of stoichiometry $ZnSnO_3$ and subjected to a 600 °C anneal; reference stick patterns for ilmenite $ZnSnO_3$ (black), and spinel Zn_2SnO_4 (grey) are superimposed. This XRD pattern is representative of the amorphous nature of zinc tin oxide films employed as TTFT channel layers with post-deposition annealing treatments up to 600 °C. (Inset) 100 000 ×SEM cross-sectional image of a zinc tin oxide thin film; the scale bar on the image is 200 nm.
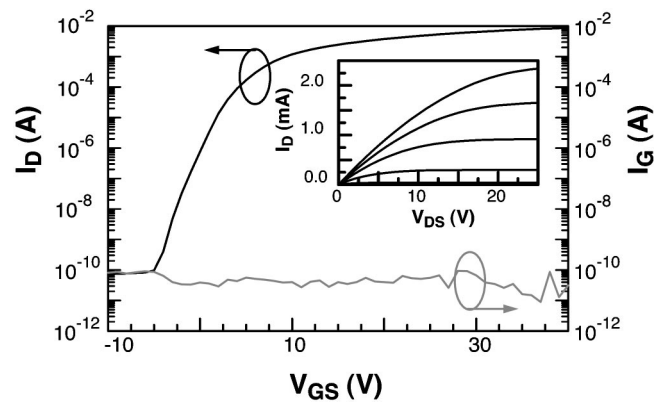
so it is not possible to explicitly identify the phase(s) present in the film. Moreover, the breadth of the diffraction peaks indicates that crystallites within the film do not exceed a diameter of ~5 nm. Thus, the exact description of the zinc tin oxide film as multiphase nanocrystalline or amorphous is difficult to discern. In contrast, above an annealing temperature near 650 °C, a multiplicity of sharp XRD peaks appear, indicating a dramatic increase in the crystalline nature of the zinc tin oxide films.

The scanning electron microscope (SEM) image shown in the inset of Fig. 2 is a cross-sectional view of a zinc tin oxide film. This image is obtained at a magnification of 100 000× and provides qualitative information regarding the morphology of these zinc tin oxide thin films. In agreement with XRD results, the image does not indicate any grain formation in the sample. Similar to the XRD results, there is little, if any, observable difference in the SEM cross-sectional view of unannealed samples and those samples that are annealed up to 600 °C.

The optical transmittance versus wavelength through the source/drain region of a zinc tin oxide TTFT is shown in Fig. 1. The average transmittance in the visible portion of the electromagnetic spectrum (400–700 nm) is ~84% for this device. The data represent raw transmission through the entire structure, including the substrate, i.e., the measured transmission is reduced by both absorption and reflection.

$\log(I_D)-V_{GS}$ and $\log(I_G)-V_{GS}$ characteristics (for V_{DS} =40 V) representative of ~50 devices with a 600 °C channel layer anneal, where I_D, V_{GS}, I_G, and V_{DS} are the drain current, gate-to-source voltage, gate current, and drain-to-source voltage, respectively, are illustrated in Fig. 3. An I_D-V_{DS} characteristic (for V_{GS}=3–15 V in 3 V steps) is shown in the inset of Fig. 3. Qualitatively, ideal TFT behavior is observed, including drain current saturation.

The electrical parameters used to characterize a thin-film transistor are typically threshold voltage, drain current on-to-off ratio, and channel mobility. The threshold voltage (extracted from an I_D-V_{GS} measurement with a small V_{DS}[21] for device operation in the linear region) is typically 0–10 V for zinc tin oxide channel TTFTs. However, precise identification of the threshold voltage for a given device is somewhat ambiguous.[21,22] A less ambiguous device parameter, although not explicitly quoted as often in the literature, is the turn-on voltage (V_{on}). V_{on} is the gate voltage at the onset of channel
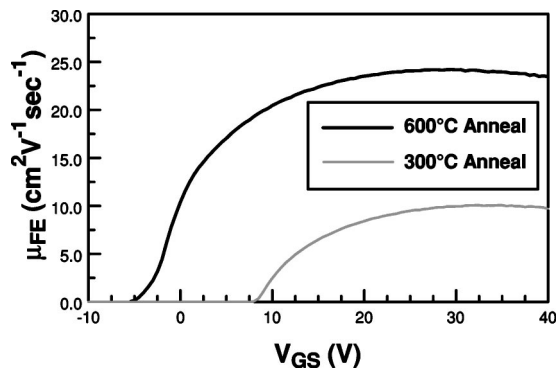
FIG. 4. Representative $\mu_{FE}-V_{GS}(V_{DS}=1$ V) characteristics for zinc tin oxide TTFTs fabricated on a Si substrate and annealed at 300 and 600 °C. The higher annealing temperature yields a higher mobility and a lower turn-on voltage.

conduction, i.e., the gate voltage at the onset of the initial sharp increase in current in a $\log(I_D)-V_{GS}$ characteristic.[22] V_{on} is equal to -5 V in Fig. 3, and it is typically -5 to 5 V for ~ 50 zinc tin oxide channel devices with a 600 °C post-deposition anneal.

The typical I_D on-to-off ratio is $\sim 10^7-10^8$. As shown in Fig. 3, the transistor "off" current is established by gate leakage, which is typically $\sim 10^{-10}$ A for the ATO gate dielectric employed here.

Channel mobility is arguably the most important TFT electrical parameter, as it quantifies the semiconductor channel layer performance, specifically with respect to current drive capability and maximum switching frequency. The channel mobility is assessed by differentiating the drain current characteristic in the linear (or triode) region of device operation, with respect to V_{GS}, i.e., the field-effect mobility (μ_{FE}).[21,22] μ_{FE} is typically 20–50 cm^2 V^{-1} s^{-1} for our zinc tin oxide TTFTs. This compares to ~ 25 cm^2 V^{-1} s^{-1} for the best polycrystalline ZnO TTFT reported to date,[22] and ~ 80 cm^2 V^{-1} s^{-1} for an engineered superlattice single-crystal TTFT prepared by pulsed laser deposition and a high-temperature anneal of 1400 °C.[5] Finally, note for comparison that opaque a-Si:H and polycrystalline-Si TFTs typically have channel mobilities on the order of 1.5–2.0 and 100–200 cm^2 V^{-1} s^{-1}, respectively.[23–25]

The zinc tin oxide channel layer has been deposited from sputter targets with two different stoichiometries, $(ZnO)_x(SnO_2)_{1-x}$ ($x=1/2$ and $x=2/3$), corresponding to the compositions of the ilmenite and spinel structures, respectively. Device performance, specifically in terms of channel mobility, exhibits little variation between these two stoichiometries, indicating the possibility of a surprising degree of insensitivity to stoichiometry (specifically the Zn:Sn ratio).

Finally, we should point out that relatively low processing temperatures, i.e., a 300 °C channel layer anneal (in place of the 600 °C anneal as discussed above), have been employed to yield devices with channel mobilities of 5–15 cm^2 V^{-1} s^{-1}, a modest performance reduction in light of the substantial decrease in processing temperature. Typical $\mu_{FE}-V_{GS}$ characteristics for devices annealed at 300 and 600 °C are illustrated in Fig. 4. This mobility trend (i.e., increasing mobility with increased annealing temperature) is tentatively attributed to modification of the semiconductor–insulator interface with annealing or improved local atomic

rearrangement at higher temperature rather than to enhanced long-range crystallinity, since zinc tin oxide films annealed at 300 and 600 °C have virtually identical XRD patterns.

The results presented in this letter identify zinc tin oxide as a viable TTFT channel layer material with respect to electrical performance and processing requirements. Furthermore, other types of amorphous oxides composed of heavy-metal cations with $(n-1)d^{10}$ns^0 $(n\geqslant 4)$ electronic configurations may provide opportunities for identification of TTFT channel materials with further improved electron transport and optical transparency.

[1] S. Masuda, K. Kitamura, Y. Okumura, S. Miyatake, and T. Kawai, J. Appl. Phys. **93**, 1624 (2003).
[2] R. L. Hoffman, B. J. Norris, and J. F. Wager, Appl. Phys. Lett. **82**, 733 (2003).
[3] P. F. Carcia, R. S. McLean, M. H. Reilly, and G. Nunes, Appl. Phys. Lett. **82**, 1117 (2003).
[4] J. Nishii, F. M. Hossain, S. Takagi, T. Aita, K. Saikusa, Y. Ohmaki, I. Ohkubo, S. Kishimoto, A. Ohtomo, T. Fukumura, F. Matsukura, Y. Ohno, H. Koinuma, H. Ohno, and M. Kawasaki, Jpn. J. Appl. Phys., Part 2 **42**, L347 (2003).
[5] K. Nomura, H. Ohta, K. Ueda, T. Kamiya, M. Hirano, and H. Hosono, Science **300**, 1269 (2003).
[6] B. J. Norris, J. Anderson, J. F. Wager, and D. A. Keszler, J. Phys. D **36**, L105 (2003).
[7] H. Hosono, N. Kikuchi, N. Ueda, and H. Kawazoe, J. Non-Cryst. Solids **198–200**, 165 (1996).
[8] H. Hosono, M. Yasukawa, and H. Kawazoe, J. Non-Cryst. Solids **203**, 334 (1996).
[9] S. Narushima, M. Orita, M. Hirano, and H. Hosono, Phys. Rev. B **66**, 035203-1 (2002).
[10] Y. Shigesato and D. C. Paine, Appl. Phys. Lett. **62**, 1268 (1993).
[11] O. Kluth, C. Agashe, J. Hüpkes, J. Müller, and B. Rech, Third World Conf. Photovolt. Energy Conversion **2**, 1800 (2003).
[12] T. Minami, H. Sonohara, S. Takata, and H. Sato, Jpn. J. Appl. Phys., Part 1 **12A**, 1693 (1994).
[13] T. Minami, H. Takata, H. Sato, and H. Sonohara, J. Vac. Sci. Technol. A **13**, 1095 (1995).
[14] T. Minami, T. Miyata, and T. Yamamoto, Surf. Coat. Technol. **108–109**, 583 (1998).
[15] D. Kovachera and K. Petrov, Solid State Ionics **109**, 327 (1998).
[16] J. D. Perkins, J. A. del Cueto, J. L. Alleman, C. Warmsingh, B. M. Keyes, L. M. Gedvilas, P. A. Parilla, B. To, D. W. Readey, and D. S. Ginley, Thin Solid Films **411**, 152 (2002).
[17] D. L. Young, Ph.D. dissertation, Colorado School of Mines, Golden, CO, 2000.
[18] D. L. Young, H. Moutinho, Y. Yan, and T. J. Coutts, J. Appl. Phys. **92**, 310 (2002).
[19] Y. S. Shen and Z. T. Zhang, Sens. Actuators B **12**, 5 (1993).
[20] ITO/ATO glass is supplied by Arto Pakkala, Planar Systems, Inc. Espoo, Finland, art_pakkala@planar. com.
[21] D. K. Schroder, *Semiconductor Material and Device Characterization*, 2nd ed., (Wiley, New York, 1998).
[22] R. L. Hoffman, J. Appl. Phys. **95**, 5813 (2004).
[23] D. W. Greve, *Field Effect Devices and Applications* (Prentice-Hall, Upper Saddle River, NJ, 1998).
[24] T. A. Voutsas, IEEE Trans. Electron Devices **ED-50**, 1494 (2003).
[25] C. R. Kagan and P. Andry, *Thin-Film Transistors* (Marcel Dekker, New York, 2003).